JGR Biogeosciences

RESEARCH ARTICLE
10.1029/2020JG006135

Special Section:
Winter limnology in a changing world

Warmer Winters Increase the Biomass of Phytoplankton in a Large Floodplain River

Kathi Jo Jankowski[1], Jeffrey N. Houser[1], Mark D. Scheuerell[2], and Adrianne P. Smits[3]

[1]U.S. Geological Survey, Upper Midwest Environmental Sciences Center, La Crosse, WI, USA, [2]School of Aquatic and Fisheries Sciences, University of Washington, Seattle, WA, USA, [3]Department of Environmental Science and Policy, University of California Davis, Davis, CA, USA

Key Points:

- Winter phytoplankton biomass was low across the river basin but comparable to summer in some areas and years
- Long-term trends were not synchronous among river reaches and habitats
- Phytoplankton biomass increased during warmer winters across the basin

Supporting Information:

Supporting Information may be found in the online version of this article.

Correspondence to:

K. J. Jankowski,
kjankowski@usgs.gov

Citation:

Jankowski, K. J., Houser, J. N., Scheuerell, M. D., & Smits, A. P. (2021). Warmer winters increase the biomass of phytoplankton in a large floodplain river. *Journal of Geophysical Research: Biogeosciences*, *126*, e2020JG006135. https://doi.org/10.1029/2020JG006135

Received 29 OCT 2020
Accepted 9 AUG 2021

Author Contributions:

Conceptualization: Kathi Jo Jankowski, Jeffrey N. Houser
Data curation: Kathi Jo Jankowski
Formal analysis: Kathi Jo Jankowski
Methodology: Kathi Jo Jankowski, Mark D. Scheuerell, Adrianne P. Smits
Visualization: Kathi Jo Jankowski
Writing – original draft: Kathi Jo Jankowski
Writing – review & editing: Kathi Jo Jankowski, Jeffrey N. Houser, Mark D. Scheuerell, Adrianne P. Smits

Abstract Winters are changing rapidly across the globe but the implications for aquatic productivity and food webs are not well understood. In addition, the degree to which winter dynamics in aquatic systems respond to large-scale climate versus ecosystem-level factors is unclear but important for understanding and managing potential changes. We used a unique winter data set from the Upper Mississippi River System to explore spatial and temporal patterns in phytoplankton biomass (chlorophyll *a*, CHL) and associated environmental covariates across 25 years and ~1,500 river km. To assess the role of regional climate versus site-specific drivers of winter CHL, we evaluated whether there were coherent long-term CHL dynamics from north to south and across lotic-lentic areas. We then estimated the degree to which these patterns were associated with climate variability (i.e., the Multivariate El Nino-Southern Oscillation Index), winter severity (freezing degree days), river discharge, or site-specific environmental variables (ice depth, snow depth, and nutrient concentrations). We found that winter CHL was typically highest in ice-free reaches and backwater lakes, occasionally exceeding summer values. We did not find highly synchronous CHL dynamics across the basin, but instead show that temporal trends were independent among river reaches and lotic-lentic areas of the river. Moreover, after accounting for these spatial dynamics, we found that CHL was most responsive to winter air temperature, being consistently higher in years with warmer winters across the basin. These results indicate that although productivity dynamics are highly dynamic within large river ecosystems, changes in the duration and severity of winter may uniformly increase wintertime productivity.

Plain Language Summary Winters are getting shorter and warmer across the globe, but how this affects rivers is not well known. This is particularly true for large rivers, such as the Mississippi River, that provide important ecological and social services at continental scales. Here, we used 25 years of data collected during the middle of winter from the Upper Mississippi River to understand long term changes in the abundance of algae, an important food resource for fish and other river organisms. We found that the quantity of algae during the winter was comparable to summer in some years and areas of the river. In addition, we found that warmer winters had more algae, which could have implications for food webs as winters change. Finally, we show that the diversity of habitats within this large river ecosystem (e.g., lakes and flowing channels) had distinct trends in algal abundance over time, providing options for consumers and helping to sustain food webs throughout the winter. Thus, our results indicate that changes in winter temperatures will have important implications for river ecosystems during winter and the rest of the year.

1. Introduction

Winter comprises a substantial fraction of the year across large areas of the globe, but what happens in aquatic ecosystems during winter is not well understood. Recent large-scale observations of decreasing ice cover (Sharma et al., 2016, 2019), warming winter temperatures (USGCRP, 2017), and increased recognition of connections between winter dynamics and conditions in other seasons (Cline et al., 2020; Collins et al., 2019; Katz et al., 2015) indicate a need to better understand the fundamental controls on winter conditions and their effects on aquatic processes and communities (Powers & Hampton,, 2017). We have made recent progress in understanding winter dynamics in lake ecosystems (e.g., Hampton et al., 2017), but we know much less about the winter ecology of rivers even though they are experiencing the same widespread increases in winter temperatures and ice loss (Prowse et al., 2011; Sharma et al., 2016; Shiklomanov & Lammers, 2014; Yang et al., 2020).

Winter can be a physically dynamic season in rivers and their watersheds (Newton et al., 2017) and substantially alter the physical template to which biological communities respond. Ice cover varies spatially and temporally as a result of flow and geomorphic conditions (Beltaos, 2003; Cooley & Pavelsky, 2016), and the type of ice that forms varies as a function of stream power and channel morphometry (Turcotte & Morse, 2013). This causes both longitudinal and lateral variation in the thickness, duration, and distribution of ice and snow cover (de Rham et al., 2008; Turcotte & Morse, 2017). This variation creates a patchwork of habitat availability and conditions within rivers through affecting light, temperature and physical disturbance (Mejia et al., 2019; Turcotte & Morse, 2017). In addition, high flow events during winter can cause substantial disturbance in river systems through breaking up ice cover, scouring sediments or causing ice jams (Nilsson et al., 2015; Rokaya et al., 2018; Tremblay et al., 2014), and have increased in recent years (Contosta et al., 2017; Rawlins et al., 2019). These dynamics have the potential to affect all levels of aquatic food webs through impacting the persistence of primary producers (Uehlinger, 2006) as well as the winter survival of fish and other consumers (Huusko et al., 2007; Knights et al., 1995; Weber et al., 2013).

How winter primary productivity responds to these factors is not well studied across river networks, and that is especially true in the largest rivers (Thellman et al., 2021, in press). A recent synthesis of annual riverine productivity regimes across the U.S. showed that although annual primary production in river mainstems typically increased with river size, productivity in small streams tended to peak in late winter or early spring but remained relatively low throughout the winter in larger rivers (Savoy et al., 2019). This pattern may not be uniform among large rivers, however. For example, annual peaks in productivity during the winter have been observed in larger reaches of some rivers (Escoffier et al., 2018; Mejia et al., 2019). In addition, winter rates of gross primary productivity (GPP) and chlorophyll *a* (CHL) concentrations were found to be intermediate between spring and summer in the large, turbid lower Mississippi River (Ochs et al., 2013). Furthermore, metabolism measured in the mainstem may have missed substantial production in off-channel areas. For instance, although production is often relatively low in the turbid, high flow environment of mainstem rivers (Hotchkiss et al., 2015; Ochs et al., 2013), the hydrogeomorphic diversity of large river-floodplain ecosystems (Amoros & Bornette, 2002; Wiens, 2002) has been shown to create opportunities for high productivity in off-channel habitats and near-shore retention zones during the growing season (e.g., Reynolds & Descy, 1996). These areas typically have longer water residence times thereby increasing water clarity through sediment deposition and promoting high primary producer biomass either as algae or macrophytes (Hein et al., 1999; Knowlton & Jones, 1997; Van den Briink et al., 1993).

Several factors may allow relatively high phytoplankton biomass and productivity in rivers during the winter. Water column irradiance sufficient for photosynthesis may occur due to high ice clarity, low snow depths, or higher water clarity resulting from reduced sediment loads from a frozen catchment and limited wind-driven resuspension under ice cover (Houser et al., 2010; Turcotte et al., 2011). This can foster productivity of algae adapted to low temperatures (Jewson et al., 2009) and that respond quickly to light availability (Twiss et al., 2014; Uehlinger et al., 2000). In addition, grazing by zooplankton and other planktivores may be lower in winter than other seasons as a result of lower temperatures, thereby releasing phytoplankton from top-down pressures (Hyrcik & Stockwell, 2020). Thus, winter phytoplankton productivity in rivers may exceed current expectations.

Phytoplankton are particularly important to large river food webs (Bukaveckas et al., 2011; Hoeinghaus et al., 2007; Thorp & Delong, 1994), thus understanding the controls on winter phytoplankton dynamics will be important in forecasting how ecosystem productivity may respond to changing winters. For instance, whether temporal dynamics of winter phytoplankton are spatially coherent can provide information about the relative strength of large scale (e.g., climate), regional (e.g., hydrological regime) and local drivers (e.g., ice cover, nutrient concentration) of their dynamics (Baines et al., 2000; Magnuson et al., 1990; Soranno et al., 2019). Climate indices such as the Multivariate El Nino-Southern Oscillation Index (MEI) have been linked to long-term dynamics in winter air temperature and snowfall, discharge, and nutrient loads within the Mississippi River Basin (Munoz & Dee, 2017; Smits et al., 2019; Twine et al., 2005). Additionally, climate-related variation in air temperature, precipitation, and solar radiation has been shown to synchronize biogeochemical variation in nutrients and CHL among lakes (Jane et al., 2017; Magnuson et al., 1990; Webster et al., 2000). Thus, these same factors could synchronize winter phytoplankton dynamics across river basins through controlling the spatial extent of ice cover or thermal conditions for growth. Conversely,

local processes may lead to asynchronous dynamics across individual rivers or lakes based on differences in their physical characteristics (Baines et al., 2000; Soranno et al., 2019), landscape setting (Marinos et al., 2020), or internal processes (Ohlberger et al., 2016). Hydrogeomorphic characteristics play an important role in structuring productivity and biogeochemical processing rates in large rivers (Houser, 2016; Ward et al., 2002), highlighting a potentially greater role of local controls that could lead to independent productivity dynamics.

To understand the patterns and drivers of phytoplankton biomass during the winter in a large river ecosystem, we used a unique, long-term midwinter chlorophyll *a* (CHL) data set (25 years) from the Upper Mississippi River System (UMRS) that spanned a ~1,500 km longitudinal gradient and a lateral (lotic-lentic) gradient within the river. We evaluated the degree to which inter-annual winter phytoplankton dynamics were coherent across the longitudinal extent and lotic-lentic gradient of the UMRS through testing models of shared behavior at several spatial scales. Specifically, we asked the following questions: (a) How does the biomass of winter phytoplankton (as CHL) vary spatially across longitudinal and lateral (lotic-lentic) gradients within the river? (b) Are there shared temporal dynamics in winter phytoplankton biomass across the basin and at what spatial scale (e.g., entire UMRS drainage basin, among river reaches, or lotic-lentic areas)? and (c) What factors are associated with inter-annual variation in winter CHL? We anticipated that the generally ice-free southern reaches of the UMRS would have greater winter CHL, and would vary independently from the ice and snow-covered northern reaches during the winter because of differences in both geomorphology and winter severity. Further, we hypothesized that CHL concentration would be low and similar between lotic and lentic areas as a result of low temperatures and reach-wide ice cover, but that the complexity of lake and riverine habitats within the river would lead to diverse and independent phytoplankton dynamics across the basin through time. Last, we expected that inter-annual variation in ice and snow cover would be key drivers of variation in winter phytoplankton biomass.

2. Methods

2.1. Site Description

The UMRS is a large, floodplain river defined as the navigable reaches of the Upper Mississippi (UMR) and Illinois (IR) Rivers. The UMR flows ~1,400 km north to south from Minneapolis, Minnesota, to the confluence with the Ohio River at Cairo, Illinois (Figure 1). It mostly consists of a continuous series of navigation pools extending from one navigation dam to the next ranging between 38 and 125 km long. The navigation dams are low-head dams built to maintain sufficient depth in the navigation channel during low-flow conditions but designed to have little effect on discharge or water level during high flow (Sparks, 1995). The locks and dams have created large, generally shallow impounded areas upstream, but their spatial extent and influence is greatest in northern UMR reaches (De Jager et al., 2018; Sparks et al., 1998). The Ilinois River connects the Great Lakes at Chicago to the Mississippi River at Grafton, Illinois and is ~439 km long. It is divided into eight navigational reaches by a series of locks and dams, which are operated differently than those on the UMR and do not create large upstream impounded areas. The broad scale (generally north-south) gradients in the UMRS are encapsulated by four "floodplain reaches" (Figure 1). These floodplain reaches are used to define spatial differences in geomorphology, aquatic vegetation and the distribution of Federal levees and include the Upper Impounded Reach (Navigation Pools 1–13), the Lower Impounded Reach (Pools 14–26), the Unimpounded Reach ("open river" pools), and the Illinois River Reach (all IR pools; USACE, 2011).

The UMRS is a useful system for understanding the causes and consequences of changes in winter conditions on river productivity. The UMRS covers a substantial north-south gradient (~8 degrees of latitude; Figure 1) resulting in a ~10°C range of average winter air temperatures (Figure 2a). In addition, the UMRS is unusual among large, developed rivers in that it also retains about half of its original floodplain. In the upper reaches, the main channel and the floodplain are well connected, even outside of impounded areas, and there are abundant connected side channels and backwaters (De Jager et al., 2018; Sparks et al., 1998). As a result, the UMRS contains a gradient of lentic and lotic areas ranging from backwater lakes to the main river channel (Bouska et al., 2018) that cover a wide range in residence time and hydraulic connectivity to the mainstem river flow. These physical differences set up gradients in water velocity (Table 1), temperature

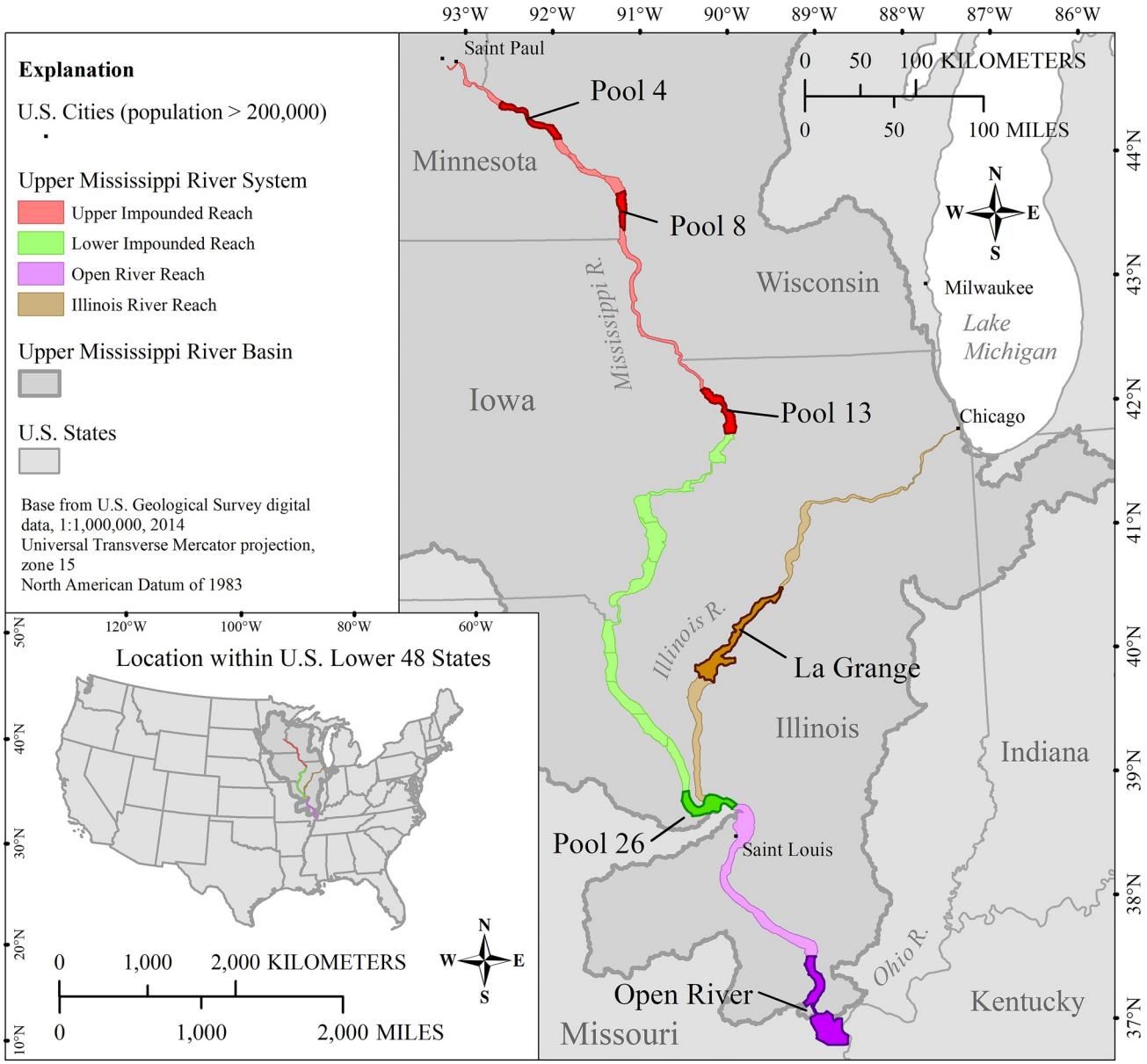

Figure 1. Map of the Upper Mississippi River System. Right panel shows a map of study reach locations and the extent of the four Floodplain Reaches. Left panel shows an example map of aquatic areas from Navigation Pool 8 near La Crosse, Wisconsin (main channel, side channels, impounded area, and backwater lakes).

(Jankowski et al., 2020), and nutrient concentrations (Carey et al., 2019; De Jager & Houser, 2012) that can influence wintertime biological productivity.

2.2. Data Collection

We used mid-winter CHL, ice, snow, and other limnological measurements collected from six reaches of the UMRS by personnel of the Upper Mississippi River Restoration Long Term Resource Monitoring element (UMRR-LTRM) from 1993 to 2018. Four aquatic area types spanning the lotic-lentic gradient were sampled per reach: backwater lakes (BW), impounded areas (IMP), side channels (SC) and the main navigation channel (MC; Figure 1). Sampling reaches in this study generally correspond to navigation pools and include Pool 4 (Lake City, MN), Pool 8 (La Crosse, WI), Pool 13 (Bellevue, IA) in the Upper Impounded reach; Pool 26 (Alton, IL) in the Lower Impounded Reach; one river reach in the unimpounded portion of the river

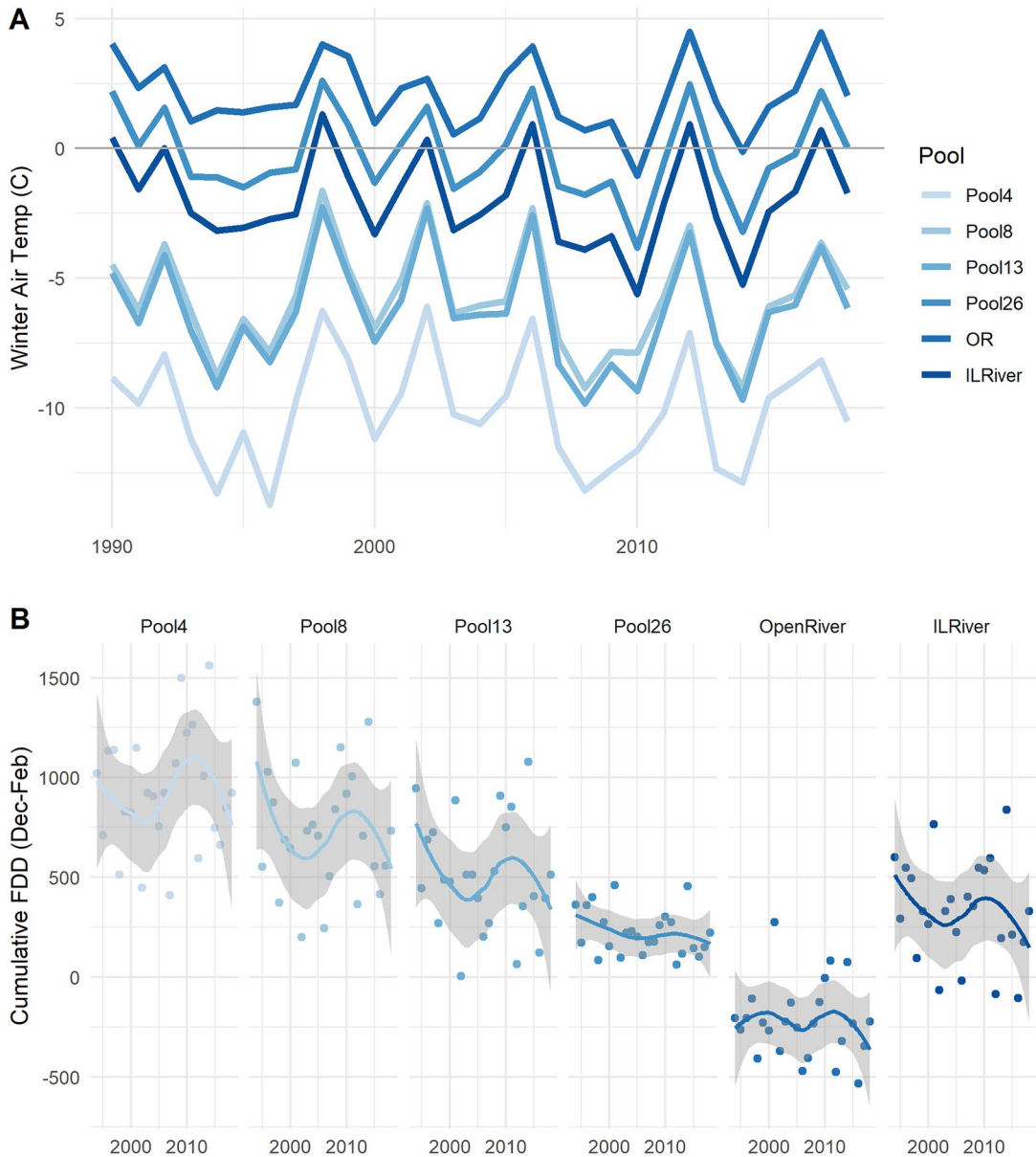

Figure 2. (a) Annual average winter air temperature from nearest weather station for each reach and (b) Cumulative freezing degree days (FDD) for 60-day period prior to last sampling date each year from 1994 to 2018. FDD data are fit with a LOESS curve to visualize variation over time. Shaded area represents the 95% confidence interval of the fitted curve.

near Cape Girardeau, MO (Open River), and one navigation pool on the Illinois River (La Grange; Havana, IL; Figure 1). Winter sampling occurred during a two-week period beginning the last full week of January. Data collection across aquatic areas followed a stratified random sampling design within each study reach (Soballe & Fischer, 2004). See Supplemental Text S1 for further description of stratified random sampling design. We compared winter CHL values to summer CHL data collected during a two-week period starting the last week of July using the same sampling design and methods.

2.3. Field Measurement and Laboratory Protocols

Ice depth at each sampling site was measured as the average of three measurements around a single hole bored through the ice with an auger. Snow depth was measured by averaging measurements at three points within an undisturbed 1-m^2 area at each sampling site. Field measurements of dissolved oxygen,

Table 1
Average Physical Characteristics for Each Study Reach and Chlorophyll Concentration by Reach and Aquatic Area Type Averaged Across All Years of the Data Set

Reach	River miles	Mean winter discharge (10^6 m^3 d^{-1})	Aquatic area	Sites per year	Average current speed (m/s)	Mean chl (ug/L)	SD	CV	N
Pool 4	1283–1212	28 ± 10	MC	25	0.25	4.5[a]	3.7	0.83	402
			SC	30	0.11	4.6[a]	4.3	0.94	465
			BW	50	0.02	8.6[b]	6	0.69	596
Pool 8	1131–1093	49 ± 19	MC	25	0.2	4.9[a]	6.6	1.36	346
			SC	30	0.12	5.4[a]	6.9	1.28	385
			BW	60	0.04	13.6[b]	8.5	0.63	524
			IMP	25	0.07	5.2[a]	6.8	1.32	321
Pool 13	896–841	84 ± 26	MC	30	0.19	4.5[a]	5.2	1.14	422
			SC	30	0.19	4.5[a]	5	1.1	448
			BW	60	0.04	13.7[b]	4.8	0.35	850
			IMP	30	0.09	5.3[a]	5	0.95	309
Pool 26	389–327	354 ± 196	MC	20	0.11	18.4[a]	18	0.98	264
			SC	42	0.36	17.9[a]	16.9	0.94	504
			BW	29	0.01	29.6[b]	13	0.44	248
			IMP	15	0.02	22.6[c]	18.2	0.81	186
Open river	129–47	411 ± 233	MC	75	0.7	13.2[a]	10.2	0.77	1143
			SC	75	0.59	12.4[a]	8.4	0.68	664
IL river	254–129	42 ± 27	MC	35		8.2[a]	6.8	0.83	494
			SC	20	0.31	8.6[a]	8	0.94	366
			BW	80	0.07	16.3[b]	13	0.8	564

Note. Letters indicate whether averages are significantly different among aquatics areas within a reach ("Mean Chl"). BW, Backwater lake; IMP, Impounded area; MC, Main channel, and SC, Side channel.

conductivity, temperature, and pH and water samples for laboratory analysis were all taken 0.2 m below the water surface or below the submerged base of the ice when present. Both water speed and direction were measured at the time of sampling using a portable velocity meter and a standard magnetic compass.

Water samples were returned to the laboratory for the determination of turbidity, total nitrogen (TN), total phosphorus (TP), dissolved silicon (DSi), and CHL. Turbidity was measured using the nephelometric method on a Hach Model 2100Q turbidity meter (Hach Inc., Loveland, CO). TN and TP samples were preserved in the field with concentrated sulfuric acid, transported on ice, and refrigerated until analysis. DSi samples were filtered in the field (0.45 μm membrane), transported back to the laboratory on ice and frozen until analysis. TN, TP, and DSi (expressed as milligrams of elemental silica per liter) were determined colorimetrically following standard methods (APHA, 2018). Further details concerning sampling design and analytical methods can be found in Soballe and Fischer (2004).

CHL was determined fluorometrically for all sites and spectrophotometrically according standard methods (APHA, 2018; see Supplemental Text S1 for method details) for a randomly chosen subset of sites (random selection of 10% of the sites sampled). Equations for deriving CHL concentrations from fluorescence were determined by regressing fluorescence against spectrophotometric CHL across the sites where both were measured. Calibration equations were determined for each year and season separately as in Houser et al. (2010).

2.4. Regional Climate and Hydrologic Variables

We used the Multivariate El Niño-Southern Oscillation Index (MEI) as an index of large-scale climate variability in our models. The MEI is an index of the cyclic variability associated with the El Niño–Southern Oscillation (ENSO) and integrates six variables describing air pressure, wind, and temperature conditions over the Pacific Ocean. Negative values indicate cold La Niña years while positive values indicate warm El Niño years. We used the winter average of three MEI values that integrated over two-month periods (December–January, January–February and February–March) and bracketed our typical sampling period (late January–early February; NOAA, 2021; https://psl.noaa.gov/enso/mei/).

Discharge data were obtained from the US Geological Survey (USGS) gaging station nearest each study reach as follows: Pool 4, station 05344500 (Prescott, Minnesota); Pool 8, station 05378500 (Winona, Minnesota); Pool 13, station 05420500 (Clinton, Iowa); Pool 26, station 05587450 (Grafton, Illinois); Open River, station 07022000 (Thebes, IL); and La Grange pool, station 05568500 (Kingston Mines, Illinois). We extracted daily discharge data from the USGS National Water Information System database (USGS, 2021) for each station from 1975-2018 for the two-month period prior to and including the sampling period (December through first week in following February). We calculated the mean of this period for each year, then normalized these data using a z-score so that yearly discharge values reflected a deviation from the long-term average (1975–2017) for each station.

We downloaded winter air temperature records from the nearest meteorological station with a continuous air temperature record using the Midwest Regional Climate Center's cli-MATE tool (mrrc.illinois.edu). We calculated both annual mean winter temperatures (December–February average) and cumulative freezing degree days (FDD). FDD provide a metric of the duration and intensity of cold temperatures and are related to the likelihood for water to freeze (National Snow and Ice Data Center; https://nsidc.org/cryosphere/glossary/term/freezing-degree-days). We calculated cumulative FDD as the sum of the average daily degrees below freezing for the two-month period prior to and including the last day of sampling each year.

2.5. Data Analysis

2.5.1. Spatial Patterns in Chlorophyll *a*

We evaluated spatial variation in winter CHL among reaches and aquatic areas using a linear mixed model to test for differences among reaches and aquatic areas that included random effects on the intercept to account for repeated sampling across years. We allowed this year affect to vary independently across reaches and aquatic areas.

We compared models with fixed effects that included reach, aquatic area, and their interaction using AICc (Burnham & Anderson, 2002) and report marginal (R^2m, fixed effects) and conditional (R^2c, full model) R^2 values for each model (MuMIn package; Barton & Barton, 2013; Nakagawa & Schielzeth, 2013). We performed pairwise comparisons among river reaches, aquatic areas and aquatic areas nested within each reach (e.g., main channel versus backwaters in Reach 1; shown in Table 1) using the "emmeans" package which calculates estimated mean differences from model outputs (Lenth, 2018).

2.5.2. Temporal Patterns and Drivers of Chlorophyll

We then used Multivariate autoregressive state space (MARSS) models to evaluate whether there were shared inter-annual CHL dynamics among our 20 reach-aquatic area time series (Holmes et al., 2014). Specifically, we evaluated (a) whether there was synchrony (i.e., shared trends) in CHL at scales ranging from the entire river basin to individual aquatic areas, (b) which environmental drivers were associated with long-term CHL dynamics, and (c) if effects of environmental variables were consistent among shared trends. The MARSS framework is a powerful means to evaluate hypotheses about synchrony among multiple time series (Ohlberger et al., 2016; Smits et al., 2019) and to partition variance in time series data between observation error and environmental stochasticity. MARSS models have two components: a process model and an observation model. The process model (1) describes changes in the true, but unobserved states of nature over time and how covariates affect each of those states. The observation model (2) relates the observed data to the unobserved states. These models are written as follows:

Table 2
Description of **Z** *Model Structures Considered in the MARSS Observation Model*

Model name	Model description	# Of state processes
UMRS	All time series followed the same trend	1
Floodplain reaches	All reaches within geomorphically defined reaches followed same trend: Groupings as follows: Pool 4+Pool 8+Pool 13, Pool 26, OR, and LG	4
Geomorphic reach/navigation pool	Each reach had a unique trend; all aquatic areas within each reach followed the same trend (six trends)	6
Aquatic area specific	Aquatic areas (BW, MC, SC, and IMP) had same trends across the river system	4
Chan/Imp and BW	Channels and impounded areas grouped by reach (six trends) and BW all unique (five trends)	11
Chan and Imp/BW	Channels grouped by reach (six trends); BW and impounded areas grouped by reach (five trends)	11
Chan-IMP-BW	Impounded areas acted separately (three trends) than Main-Side channels (six trends) and backwaters (five trends) in each reach	14
All unique	All time series followed independent trajectories	20

Note. Models compared groupings of CHL time series at different spatial scales ranging from the entire UMRS basin to individual aquatic area types within reaches of the river.

$$\mathbf{x}_t = \mathbf{B}\mathbf{x}_{t-1} + \mathbf{C}\mathbf{c}_{t-h} + \mathbf{w}_t; \mathbf{w}_t \sim \mathrm{MVN}\left(0, \mathbf{Q}\right) \quad (1)$$

$$\mathbf{y}_t = \mathbf{Z}\mathbf{x}_t + \mathbf{v}_t; \mathbf{v}_t \sim \mathrm{MVN}\left(0, \mathbf{R}\right) \quad (2)$$

In the observation model (3), $\mathbf{y}_t$ is a $i\ x\ 1$ vector of measured CHL values for each of the reach-aquatic area combinations at time t ($i = 20$). The matrix, **Z**, maps each observed time series onto the hidden states estimated as $\mathbf{x}_t$ (i.e., the true, but unobservable CHL concentrations). The number of states is not necessarily equal to the number of time series; rather, the number of states can be manipulated to test whether there are shared trends across time series (e.g., compare models with one to 20 trends). To address our first question, we designed several **Z** matrices that allowed us to test the degree of temporal coherence at different spatial scales across the UMRS, from the entire basin to individual reach-aquatic area combinations, by mapping the observed time series onto 1–20 hidden states. We considered the following site groupings: (a) Entire UMRS basin, (b) Floodplain reaches, (c) Study reaches, (d) Aquatic area specific, (e–g) Lotic-lentic differences, and (h) All independent (see Table 2 for further description of site groupings). Lotic-lentic models were designed to test whether there was coherence among certain aquatic area types within study reaches and included different groupings of aquatic areas: (e) Impounded grouped with channels, backwaters independent, (f) Impounded grouped with backwaters, channels separate, and (g) Impounded, backwaters and channels all independent. In the observation model (2), the $i \times 1$ vector $\mathbf{v}_t$ contains the observation errors, which are distributed as a multivariate normal (MVN) with mean vector 0 and covariance matrix **R**. Because the same collection and analysis methods were used for all samples, we modeled **R** as "diagonal and equal," meaning that the variance among observation errors was equal across all time series. Both the observed CHL data and the covariates were standardized to have a mean of 0 and standard deviation of 1 to facilitate model comparisons and interpretation across sites and spatial scales.

In the process model (1), $\mathbf{x}_t$ is a $j\ x\ 1$ vector of states in year t. The diagonal elements of the $j \times j$ matrix **B** determine the degree of mean-reversion of each state process, which we considered to be equal among states. **C** is a $j\ x\ k$ matrix that maps the effects of k external drivers (covariates) measured at time t-h onto the states. h represents the time lag between the covariate and the response. Here, we set h to zero assuming that covariate data from the same year would better describe variation in CHL than data from the year prior. In addition, this matrix allows the effects of covariates to vary among states (e.g., correlation between TP and chlorophyll could differ between reach 1 vs. reach 2). The **c** vector ($k\ x\ 1$) contains each of the measured covariate values at the scale appropriate to each modeled state. The $j\ x\ 1$ vector $\mathbf{w}_t$ contains process errors which are distributed as multivariate normal with mean vector **0** and covariance matrix **Q**. We evaluated five options for the **Q** matrix to model the variance and possible covariance among state processes: (a) equal variance and equal covariance, (b) independent variance but no covariance, (c) equal variance but no covariance, (d) independent variance and independent covariance, and (e) "custom **Q**"—independent

variance, but only relevant longitudinal and lateral covariance was estimated (Table S1). The off-diagonals of the **Q** matrix measure covariance in the process errors after accounting for the effects of the covariates, thus providing another estimate of shared behavior. We report values from the **Q** matrix as correlations for ease of interpretation. We used AICc to select the model with the number of states (**Z** matrix) and process error (**Q** matrix) that had the most support from the data (Burnham & Anderson, 2002) as suggested by Zuur et al. (2003). It is important to note that we used the values of the Q matrix after evaluating and selecting the best covariate structure as described below. It is possible, however, that the addition of different or additional covariates could affect the degree of covariance among state processes if that covariation is better captured by another environmental factor not included in the best model. Thus, these values are best interpreted as the degree of shared variation after accounting for the effect of the most influential covariate but could change if other influential variables were added.

To test among potential drivers of CHL dynamics and evaluate hypotheses regarding whether CHL responded similarly to drivers in all locations, we used the model structure selected above and adjusted the **C** matrix in the process model (1) to map covariates to state processes. We compared models that included nine potential covariates: MEI, discharge (Q), FDD, ice depth, snow depth, water temperature, TN, TP, or DSi. Given the large number of possible models, we ran models that included only a single predictor but compared two **C** matrix options in each case for a total of 18 models: (a) Shared effect: all state processes responded the same way to each covariate (one coefficient), and (b) Separate effects: each state process had unique responses to covariates (number of coefficients = number of states; Table 2). We hypothesized that given different phytoplankton community composition from north to south and across the lotic-lentic gradient (Manier et al., 2021), their response to nutrients or other drivers may also differ among sites. Model residuals were examined for normality, autocorrelation and homogeneity. We evaluated correlations among individual covariates, which are shown in Tables S4 and S5.

Concentrations of CHL and nutrients below the analytical detection limit were set to half that value (see Soballe & Fischer, 2004 for values) and data were log-transformed prior to analysis to meet assumptions of normality where necessary. All analyses were done using R version 4.0.3 (R Core Team, 2020).

3. Results

3.1. Physical-Chemical Conditions

Mean winter discharge ranged from 28 to 411 10^6 m^3 d^{-1}, increasing ~15-fold between Pool 4 and the Open River. Average winter air temperatures were consistently below freezing for Pools 4, 8 and 13, but above freezing during seven years for Pool 26 and LG and for most years for Open River (Figure 2a). Average freezing degree days (FDD) ranged from 924 (Pool 4) to −224 (Open River; Figure 2b). These north-south air temperature patterns were associated with markedly higher ice thickness, on average, in the three northern reaches than in the three southern reaches, ranging from a maximum of 27.1 cm in Pool 8 to a minimum of 0 in Open River (Figure 3). A similar pattern occurred for snow depth; the Open River reach had minimal snow cover (<1 cm) and Pool 8 had the maximum long-term average of 5.87 cm. Similar to summer conditions in the UMRS (Carey et al., 2019; Houser et al., 2010), total N and P generally increased and DSi decreased downriver within the UMR. The highest average values of N and P and lowest values of DSi occurred in the IL River (Figure 3), however, which meets the UMR near St. Louis and flows into Pool 26.

Ice depth, snow depth and nutrient concentrations also differed across the lotic-lentic gradient. Ice and snow depths were greater in slower flowing areas (i.e., backwaters and impounded areas) than in channels (i.e., main and side channels; Figure 3). Maximum ice and snow depths were in Pool 4 backwaters and minimum in the Open River Reach main channel, which never had stable ice cover during the period of record. Nutrient patterns differed across the lotic-lentic gradient during winter: although TN and DSi were consistently lowest in backwaters across all reaches, lotic-lentic patterns in TP were more variable. TP was lower in backwaters than the main channel for Pool 26 and LG but similar to or higher in backwaters than the main channel in Pools 4, 8, and 13 (Figure 3).

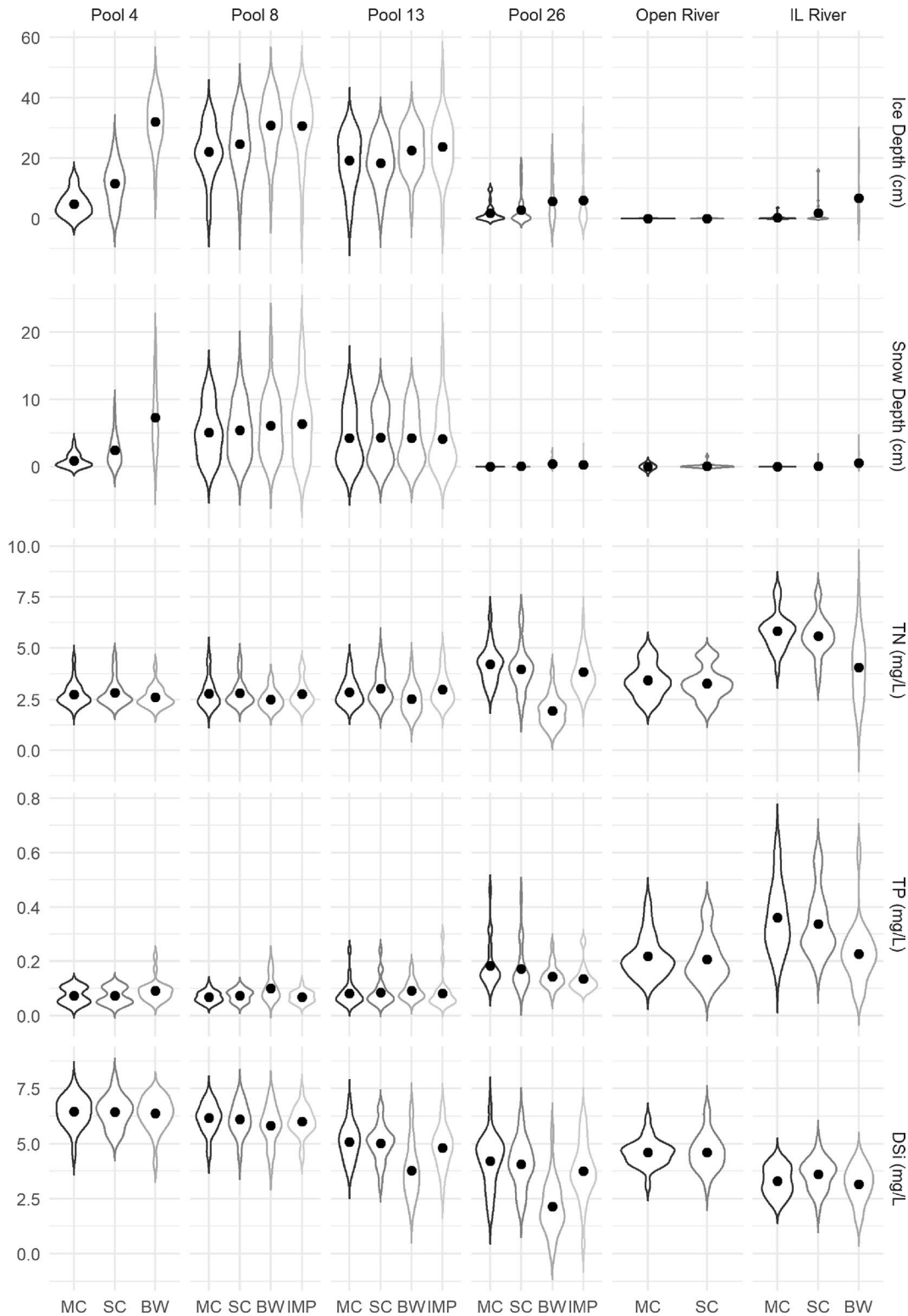

Figure 3. Mean and distribution among reaches and aquatic areas of covariates measured at the site scale: ice depth (cm), snow depth (cm), Total Nitrogen (TN, mg/L), Total Phosphorus (TP, mg/L), and Dissolved silicon (DSi, mg/L). MC = main channel, SC = side channel, IMP = impounded area, and BW = backwater lake.

3.2. Spatial Patterns in CHL

Average annual winter CHL concentrations ranged from below detection (<1 μg/L) to 71.2 μg/L across all years and reaches (Table 1, Figures 4a and 5a). CHL generally increased from north to south: the three northern reaches had lower CHL on average across all aquatic areas over the period of record (Pool 4: 4.5–8.6 μg/L, Pool 8: 5.2–13.6 μg/L, and Pool 13: 4.5–13.7 μg/L; Table 1) than the two southern reaches (Pool 26: 17.9–29.6 μg/L, Open River: 12.4–13.6 μg/L) and the IL River (8.2–16.3 μg/L; Tables 1 and S2). Winter CHL ranged between 18% and 64% of summer CHL on average for each reach-aquatic area combination. However, winter CHL was observed to exceed summer CHL at least once in all study reaches and, in some years and areas, winter CHL reached up to 2.3 times summer CHL (Figure 4b). The highest winter values consistently occurred in Pool 26, with significantly higher concentrations than all other reaches except Open River (pairwise differences among estimated means were all $p < 0.001$, Table S2; Figures 4b and 5a). Lotic-lentic differences in CHL were generally consistent across reaches, but lower in the winter than in the summer (Figure 4c). The highest concentrations consistently occurred in backwater lakes, with similar concentrations between impounded areas and channels (Table 1, Figures 4a and 4b). Finally, although spatial variation was typically highest among backwater lakes within any given year (e.g., Figure 4a), inter-annual variability in winter CHL was higher in channels and impounded areas than backwater lakes (CV in Table 1, Figure 5a).

3.3. Temporal Dynamics of Phytoplankton Biomass

We found that winter CHL dynamics were largely independent across reaches and the lotic-lentic gradient of the UMRS. A lotic-lentic model ("Chan/Imp and BW," Table 2) was the most supported by the data (Table S4, Figure 5b). This model included 11 unique CHL trends that separated higher flow areas (i.e., main channels, side channels and impounded areas) from backwater lakes in each reach (Table 2, Figure 5b). There were no other models within 10 AICc units of this lotic-lentic model, and it was substantially better than models that assumed shared dynamics at larger or finer scales (Tables 2 and S4). Interestingly, we found that there was not strong support for impounded areas having independent dynamics from other aquatic areas ("Chan-Imp-BW" model, Table 2) or for behaving similarly to backwater lakes ("Chan-IMP/BW" model, Tables 2 and S4).

These results indicate that CHL dynamics were not highly synchronized longitudinally across the UMRS despite being connected by north-south flow or across lotic-lentic gradients by hydraulic exchange. However, our model results also indicated that there were important differences in the magnitude of shared behavior across reaches and among aquatic areas, as indicated by the process error structure of the best-fitting model (**Q** matrix, Table 3), and in CHL time series shown in Figure 4a. We found that estimating covariance independently across a specific subset of state processes focused on longitudinal and lateral connections performed best ("custom" **Q** matrix shown in Tables S1, S4, and 3) and allowed us to further explore the shared behavior among reaches and aquatic areas. Specifically, we used covariance estimates from this **Q** matrix to assess whether dynamics were more correlated among reaches that were closer together and if correlations between lotic-lentic areas varied across reaches (e.g., do channels and backwaters covary more strongly in Pool 4 than in Pool 26?). We found that dynamics among channels in the southern reaches (Pool 26, Open River, and IL River) were more correlated than those in northern reaches, with channels of the IL River and the OR reach showing the highest correlations ($r = 0.87$), followed closely by Pool 26-OR and Pool 26-IL River ($r = 0.86$ and 0.76, respectively). The pattern differed correlations between channels and backwaters in the same reach however. We found that channels and backwaters in the IL River, Pool 4 and Pool 8 were more highly correlated ($r = 0.84$, 0.85, and 0.78, respectively) than those in Pools 13 and 26 ($r = 0.08$ and -0.06, respectively; Figure 5).

Among all the environmental covariates, we found that FDD best explained inter-annual patterns in CHL (Table S7, Figure 6). No other drivers had a high degree of support (ΔAIC > 10 compared to next best covariate; Table S7), but the next best models included either a shared, negative effect of Q or a separate effect of DSi across all states. FDD had a uniformly negative effect on CHL (Figure 6; mean/std deviation: -0.30 ± 0.06, 95% Confidence Interval (CI): -0.33, -0.28), indicating that colder winters reduced phytoplankton biomass similarly across the extent of the UMRS (Figure 7a).

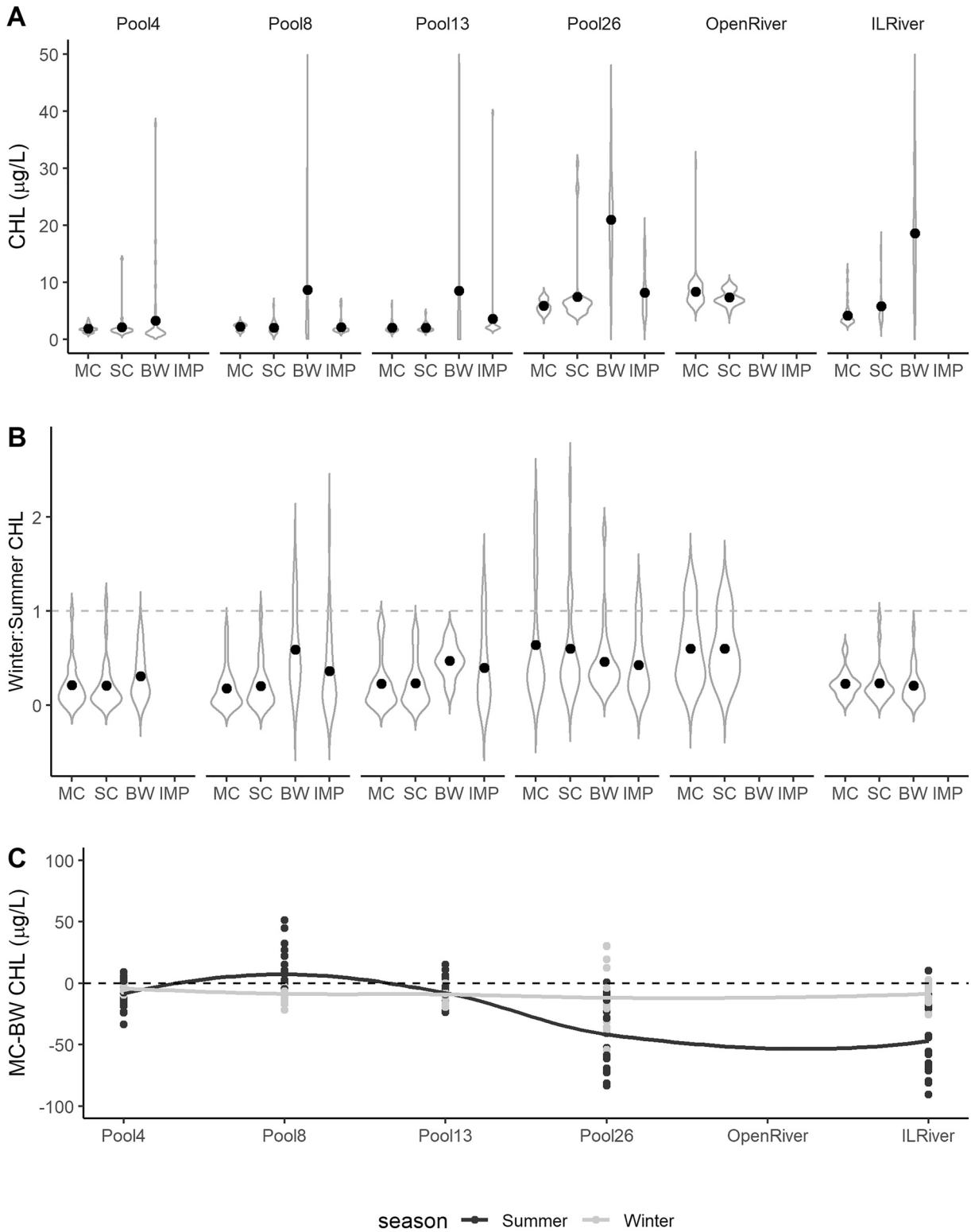

Figure 4. (a) Spatial variation within aquatic areas for a single representative and recent year (2017), (b) Ratio of winter chlorophyll (CHL) to summer CHL for all study reaches and aquatic areas. Vertical black line indicates ratio = 1, and (c) Difference between main channel and backwater CHL among reaches in the summer and winter. Data are fit with a LOESS smoother to show the seasonal contrast in the magnitude of lotic-lentic differences. Black points represent means in panels a and b; "MC" = main channel, "SC" = side channel, "BW" = backwater lake, and "IMP" = impounded area.

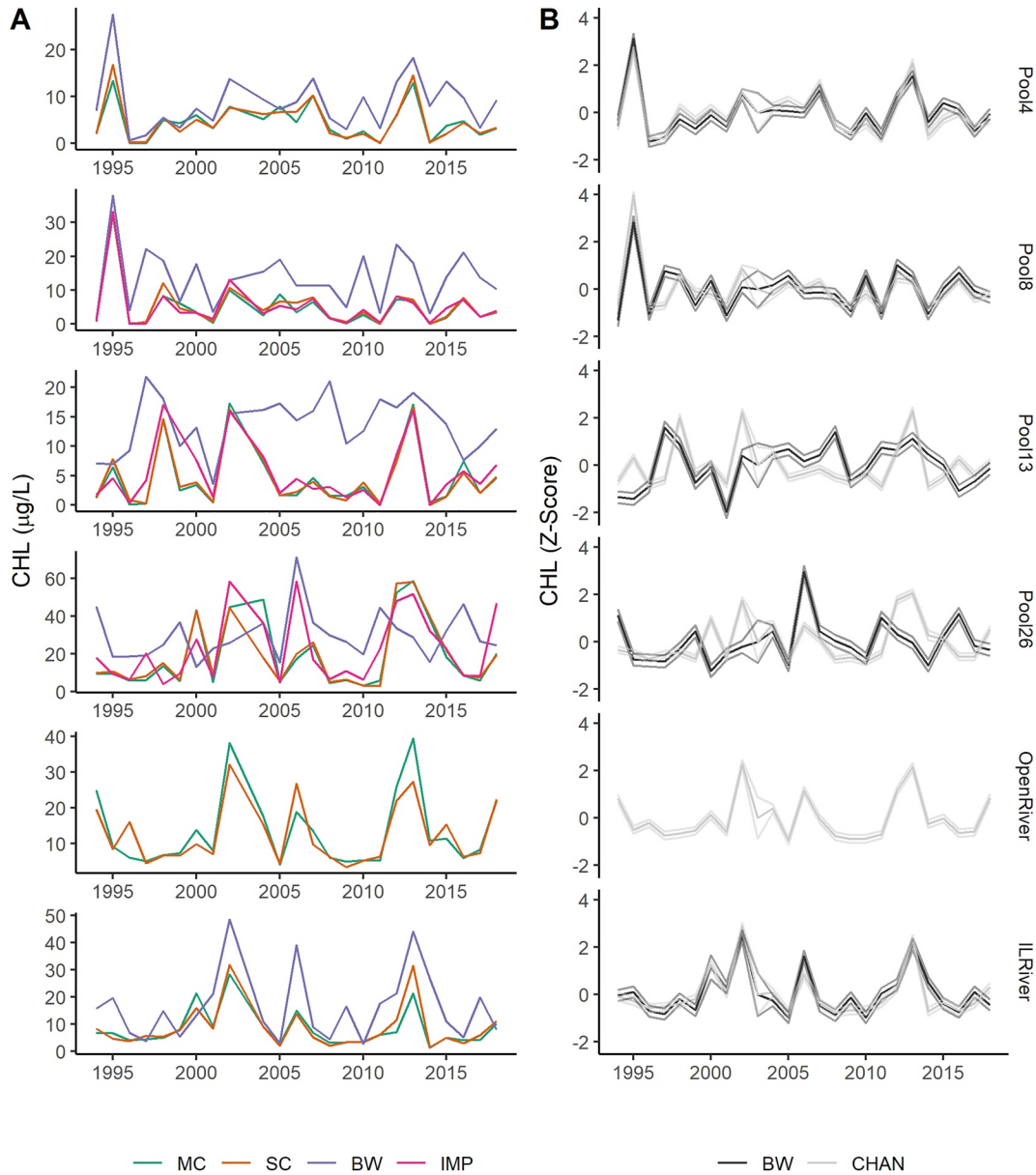

Figure 5. (a) Annual average winter CHL for all aquatic areas in each study reach from 1994 to 2018 and (b) Estimated MARSS model states from the most supported model—"CHAN/IMP and BW." Black = backwater lakes and Blue = main channel/side channel/impounded areas. Estimates are shown with their standard error.

4. Discussion

Our understanding of productivity patterns in rivers is primarily based on observations during the summer season, but we find that the biomass of river phytoplankton can be comparably high in some areas and times during the winter. In addition, we found that although the biomass of phytoplankton varied substantially in space and time across the large and dynamic river basin of the UMRS, warmer winters consistently supported greater phytoplankton biomass throughout the river, indicating that riverine phytoplankton will be sensitive to shifts in winter air temperatures. We hypothesized that the presence of ice cover during the winter would reverse the longitudinal pattern and decrease the lotic-lentic differences in CHL typically observed during summer (Carey et al., 2019; Crawford et al., 2016; Houser, 2016; Houser et al., 2010), expectations which we largely confirmed. However, we also expected that there would be similar CHL temporal dynamics among areas in ice covered versus ice free reaches (i.e., north versus south), but found that

Table 3
*Estimates of Individual Correlations Among Reaches and Between Channels and Backwaters Within Reaches From Process Model Variance-Covariance (**Q**) Matrix*

Type	Reach	Distance (km)	Mean
Lateral (channel-backwater)	p4	n.a.	**0.85**
	p8	n.a.	**0.78**
	p13	n.a.	0.08
	p26	n.a.	−0.06
	IL	n.a.	**0.84**
Longitudinal (channel-channel)	p4-p8	81	**0.72**
	p4-p13	316	**0.50**
	p8-p13	197	**0.29**
	p26-OR	198	**0.86**
	p26-IL	129	**0.76**
	IL-OR	327	**0.87**

Note. Significance is indicated in bold where CI did not cross zero.

inter-annual CHL dynamics were independent among all reaches and between lotic and lentic areas. This demonstrates an important role of river hydrogeomorphology for structuring productivity dynamics even in winter, emphasizes the need to consider habitat diversity when measuring large river productivity, and indicates that there will be considerable complexity in how large rivers respond to changing winters.

4.1. Spatial Patterns in Winter CHL

Midwinter CHL was expectedly low compared to other seasons in the UMRS (Burdis et al., 2020; Carey et al., 2019; Houser et al., 2010, 2015), but similar to winter CHL measured in other freshwater systems (Hampton et al., 2017; Twiss et al., 2014) and in the lower Mississippi River (9–12 μg/L; Ochs et al., 2013). On average, winter CHL ranged between 18% and 64% of summer CHL, with the higher ratios occurring in southern reaches and backwater lakes. Interestingly, however, winter CHL exceeded summer CHL in at least one year in all reaches, occurring most frequently in backwater lakes. Although evidence that phytoplankton may disproportionately increase pigment concentrations during winter months to increase their capacity to quickly respond to patchy light availability means that comparisons of CHL across seasons should be viewed with some caution (Hampton et al., 2017), these results indicate that high abundances of phytoplankton can occur during the winter in large rivers.

Winter CHL varied substantially across both longitudinal and lateral gradients in the UMRS. We observed a nearly 4-fold increase in algal biomass downstream, which contrasts with declining patterns observed during the rest of the year in the UMRS and other large, turbid floodplain rivers (Crawford et al., 2016; Houser et al., 2010). This could be due to a number of factors. In many large floodplain rivers, especially eutrophic rivers such as the UMRS, phytoplankton are often more limited by light (Bukaveckas et al., 2011; Ochs et al., 2013) and variable flow conditions than nutrients (Manier, 2015; Sellers & Bukaveckas, 2003). Given winter nutrient conditions remained high, it is likely that the increasing downstream CHL reflects the gradient in winter conditions from north to south that affect water column light conditions, with greater ice and snow cover in the north and open water in the south. Thicker ice cover is more likely to impede light penetration, can reduce available water depth in shallow areas, and may indicate longer duration ice cover, thereby reducing photosynthetic potential and affecting nutrient availability over the longer term (Magee & Wu, 2017; Powers et al., 2017). In addition, turbidity declined substantially throughout the river during the winter compared to summer (Figure S1). Although winter turbidity declines in southern reaches were smaller than in the north, southern reaches were substantially less turbid than during the summer and had inconsistent ice or snow cover thereby allowing for more abundant light for photosynthesis. Thus, the longitudinal winter temperature gradient and resulting southern extent of ice cover on the UMRS may have important implications for the basin-wide magnitude of winter production.

Backwaters supported greater CHL than channels in all reaches, even though mean ice thickness was greater in lentic than lotic areas. Longer residence times, warmer temperatures and higher water clarity typically make lentic areas more hospitable to planktonic organisms during the summer (Cole et al., 1992; Houser, 2016; Knowlton & Jones, 1997), conditions which remained consistent during winter. In addition, high clarity ice without snow cover can allow substantial light penetration into the water column, which can decouple the relationship between ice thickness and under-ice production in some cases (Sharma et al., 2020). Finally, backwater areas are also likely to be more protected from scouring flows, ice jams, or other disturbances that limit productivity in faster flowing river channels during winter (Uehlinger & Naegeli, 1998).

4.2. Are There Shared CHL Dynamics Across the UMRS?

Shared CHL dynamics at large scales (e.g., UMRS basin or floodplain reaches) would imply that phytoplankton communities were responding to similar drivers that acted across the entire basin (e.g., MEI). Our

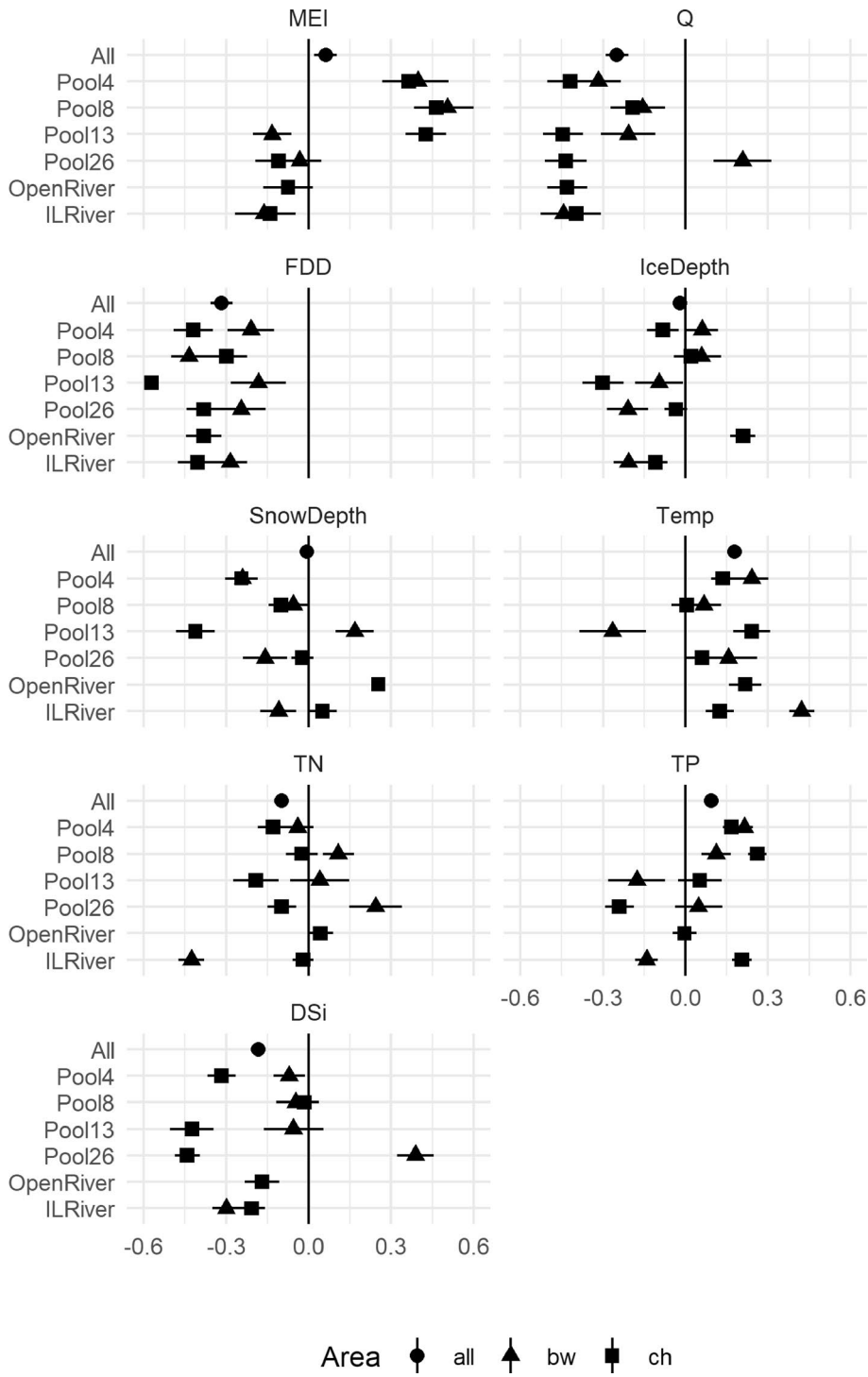

Figure 6. Estimated mean and bootstrapped confidence intervals of MARSS model coefficients for each single covariate model considered. Each panel includes the estimate of the shared coefficient ("All," circles) and coefficients estimated separately for main channel/impounded (square) and backwater (triangle) states. MEI = Multivariate El Niño-Southern Oscillation Index, Q = discharge, FDD = freezing degree days, IceDepth = ice thickness, SnowDepth = snow depth, Temp = water temperature, DSi = dissolved silicon, TN = total nitrogen, TP = total phosphorus.

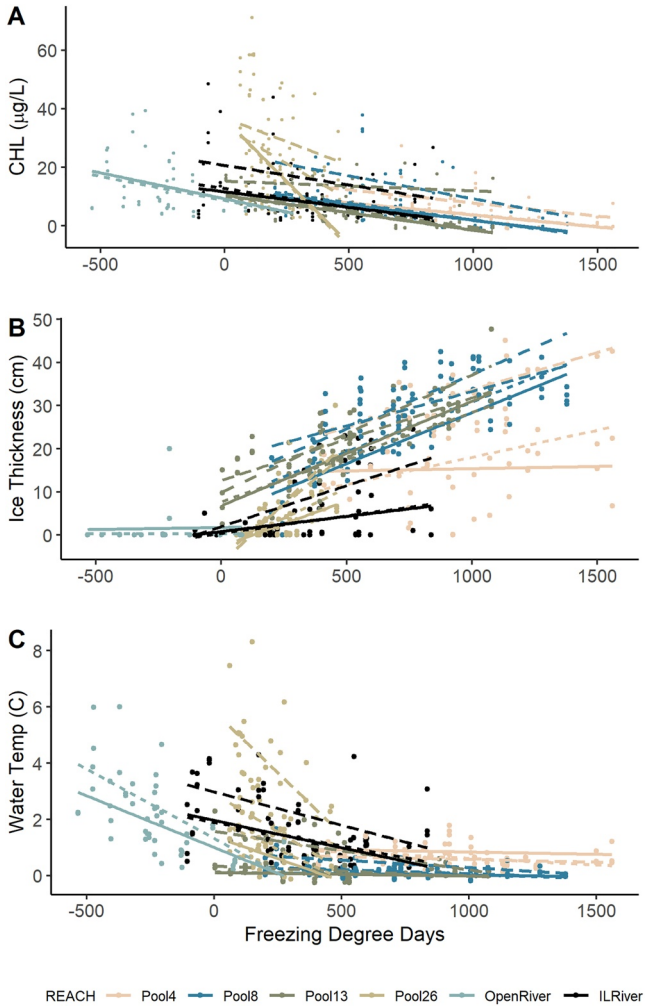

Figure 7. Relationship of (a) chlorophyll, (b) ice thickness and (c) water temperature related to freezing degree days across reaches and aquatic areas. Colors of points and lines indicate reaches and line styles indicate aquatic areas (solid = MC, short dash = SC, longdash = BW, and dotdash = IMP).

results did not support this hypothesis, however, demonstrating instead that dynamics varied at a smaller spatial extent, varying independently among reaches and across the lotic-lentic gradient. This agrees with previous work showing that annual productivity regimes are asynchronous within river networks and respond to more local scale variation in watershed characteristics (Mejia et al., 2019). We also expected that longitudinally connected reaches would have similar CHL dynamics, especially among northern reaches that had similar ice cover dynamics, but our results showed that the upstream-downstream connections among these reaches were not strong enough to synchronize mid-winter CHL at the spatial extent evaluated in this study. If these upstream-downstream connections were stronger, we would have expected the "Floodplain Reaches" model to have more support, given that those reaches are defined by common physical features, geological histories (Figure 1; Lubinski, 1993), and similar ice and snow conditions (Figure 3). Instead, our results consistently showed that differeces among reaches were important, indicating that finer scale differences influenced winter phytoplankton dynamics even in a connected riverine environment. Further, we did not find decreasing levels of covariance among river reaches that were more geographically distant (Table 3). CHL dynamics were more correlated among the southern reaches—Pool 26, OR and LG—than among northern reaches—Pools 4, 8, and 13—which are closer together. Southern reaches generally have greater longitudinal connection as measured by days that lock and dam gates are out of the water (Bouska et al., 2019) and had less frequent ice cover in our study (Figure S2), increasing potential for greater north-south hydrological connection. In contrast, the northern reaches have more physical habitat complexity (as measured by the portion of their area as contiguous backwaters; De Jager et al., 2018), which may lead to more local control of their productivity dynamics and greater differences among reaches.

Winter CHL dynamics were also independent across the lotic-lentic gradient each river reach. Specifically, CHL dynamics in backwater lakes were distinct from dynamics in channels and impounded areas. This complements the differences we observed in long-term average CHL concentrations (Table 1) and suggests the hydrological (e.g., flow velocity and connectivity) and geomorphic (e.g., depth) differences across the lotic-lentic gradient of the river led to distinct biological dynamics even during a season of the year typically characterized by slow biological rates. Interestingly, the best model grouped CHL dynamics in impounded areas with channels rather than backwaters (Table S4). Although impounded areas in the UMRS have shorter residence time than typical river impoundments (Sparks, 1995), they tend to have flow velocities similar to backwaters (Table 1). In addition, other studies have shown that they have similar phytoplankton (Manier et al., 2021) and vegetation communities (Moore et al., 2010) to backwaters during the growing season. Thus, we anticipated long-term CHL dynamics in impounded areas may behave more similarly to backwaters. Our results indicate that this was not the case, however, and that as vegetation communities senesce, the slightly higher flow in impounded areas makes them more like channels during the winter in terms of pelagic production.

Divergent dynamics of CHL and water clarity caused by ecosystem-scale physical differences have been widely shown in lakes (Lottig et al., 2017; Soranno et al., 2019). For example, in a study of small lakes across northern Wisconsin (USA), CHL dynamics in strongly stratified lakes were more synchronous than those with weak stratification (Baines et al., 2000). This occurred independently of their geographic separation and was linked to how stratification intensity influenced the importance of external versus internal nutrient loads in fueling epilimnetic production, which varied with lake physical characteristics. Independent dynamics between backwaters and channels in the UMRS likely result from their distinct hydrology, with

backwaters having slower, more stable flow dynamics, thicker ice and snow cover, and differences in nutrient concentrations (Figure 3). Interestingly, we also found that the degree of covariance across the lotic-lentic gradient varied among reaches, being strongest in Pools 4, 8 and La Grange, and weakest in Pools 13 and 26. Reaches in the Upper Impounded reach (Pools 4, 8, and 13) tend to have greater lateral connectivity (Bouska et al., 2019), which could explain this greater degree of covariance, at least for Pools 4 and 8.

4.3. What are the Drivers of Inter-Annual Variation in Winter CHL?

We found that CHL was highest in years with warmer winters, indicating that trends toward warmer and shorter winters could affect the productivity of the UMRS and other large rivers. Despite this uniform effect of winter temperature, our results indicated that the mechanisms underlying this relationship differed across the UMRS. Colder, more severe winters (as indicated by FDD) can influence several aspects of the river environment that affect phytoplankton, namely ice cover and water temperature. Our results show that these manifested differently across the eight-degree latitudinal gradient of the river. In northern reaches, FDD were strongly related to measured ice thickness values (Table S5; Figure 7), whereas FDD better described water temperature changes in southern reaches that were more frequently above freezing. Surprisingly, despite this strong influence of winter temperature on CHL, ice and snow cover variables were never among the best models of CHL dynamics. This likely relates to the more limited spatial and temporal scale of our measured snow and ice variables versus regional air temperatures captured by FDD. For instance, our measurements of ice and snow depth reflected more site-specific and short-term snapshots of ice conditions whereas FDD likely integrated several aspects of ice cover over a greater portion of the upstream watershed such as ice duration and spatial extent. In southern reaches, FDD were closely related to water temperature. Colder water temperature can slow algal metabolism (Allen et al., 2005) and rates of nutrient cycling (Richardson et al., 2004) and thereby affect total community abundance. These results show that an integrative metric such as FDD is likely to better capture the spatial variation in winter across a large river like the UMRS. Further, this relationship indicates that both reduced ice cover and warmer winter water temperatures could increase the biomass of phytoplankton as winters warm.

Although FDD best described CHL dynamics, there were some interesting patterns that fell out among the next best models. First, discharge was the next best covariate and had a shared, negative effect on CHL concentrations (C: Mean = −0.26, SD = 0.07, Figure 6, Table S7). Hydrology is typically a dominant control of biogeochemistry and productivity in large floodplain rivers (Hein et al., 1999; Knowlton & Jones, 1997; Van den Briink et al., 1993) and has important influences on phytoplankton community composition (Decker et al., 2015; Hein et al., 1999; Manier, 2015), metabolic rates (Hall et al., 2016; Houser et al., 2015; Sellers & Bukaveckas, 2003), and algal biomass (Houser, 2016; Ochs et al., 2013) in large rivers. The negative effect of discharge on CHL implies that higher winter discharge either may have acted uniformly to decrease light availability through increased turbidity (Sellers & Bukaveckas, 2003) or to decrease residence time and flush phytoplankton or nutrients downstream. Second, we observed a stronger relationship of DSi with CHL dynamics than with TN or TP. This varied across the lotic-lentic gradient, with backwaters exhibiting either a positive (Pool 26) or less negative relationship (Pools 4 and 13) with DSi than channels. Diatoms are a substantial component of large river phytoplankton communities (e.g., Kireta et al., 2012) and are often more abundant in main channel than backwater habitats during the growing season in the UMR (Manier, 2015), which may explain this pattern. Diatoms and supplies of DSi have been shown to be particularly important for winter lake communities. For example, studies in Lake Baikal demonstrated that the long-term oscillation in winter phytoplankton biomass was linked to climate signals that affected fall concentrations of DSi, implying that supplies of DSi may be especially important to consider for winter productivity if it is dominated by diatoms (Katz et al., 2015; Twiss et al., 2012).

There are some additional factors that should be considered when interpreting our results. Our winter sampling was restricted to a two-week period during late January–early February to represent mid-winter conditions across the UMRS. However, the timing of winter peak CHL may change from year to year based on ice onset and duration, high flow events or changes to winter temperatures (e.g., Katz et al., 2015). Therefore, our annual winter measurements represent different stages of the development of algal communities from year to year. Similarly, the time horizon of our covariates either represent snapshot conditions during the two-week winter sampling period (ice, snow, TN, TP, and DSi) or a two-month window prior to the

sampling event (Q, FDD). Thus, we are not capturing all aspects of previous summer and fall conditions that may influence the progression of phytoplankton communities such as aquatic vegetation biomass, nutrient loads, or fall high discharge events. In general, there remains a need for better understanding the timing of and controls on the development of algal communities over the course of the winter in rivers (Kendrick & Huryn, 2015; Uehlinger, 2006). In addition, as a metric of algal biomass, CHL is not equivalent to rates of productivity and the strength of the relationship between CHL and gross primary production in the Mississippi River is variable (Houser et al., 2015; Ochs et al., 2013). A better understanding of the relationship between winter algal biomass and water column GPP is needed. Finally, production in large floodplain rivers is often dominated by phytoplankton, thus these results may not translate well to rivers dominated by benthic productivity. Further evaluation of how the magnitude and dynamics of winter productivity vary with river size and transitions from benthic to pelagic productivity will improve our understanding of how watersheds function throughout the year.

5. Conclusions

Here, we provide one of the first long-term perspectives on the dynamics and drivers of winter phytoplankton biomass in a large river ecosystem. We provide evidence that winter productivity is likely a more important component of annual productivity than previously understood and will respond to changes in winter ice and thermal regimes. Further, longitudinal and lateral differences in chlorophyll dynamics demonstrate the potential ecological importance of the current diversity of habitats within this large river ecosystem for sustaining productive winter food webs. We also show that CHL dynamics were most strongly associated with the severity of winter, implying that shifts in winter temperatures and snow and ice phenology will have important implications for winter phytoplankton abundance in the UMRS and other river ecosystems. Thus, how a changing climate affects winter temperature and the resulting extent and duration of ice cover within large river watersheds could have important implications for the basin scale magnitude of winter and annual production.

Data Availability Statement

Data used in this manuscript are available for download here: https://umesc.usgs.gov/data_library/water_quality/water_quality_data_page.html.

Acknowledgments
K. J. Jankowski and J. N. Houser were supported by the US Army Corps of Engineers Upper Mississippi River Restoration Program. A. P. Smits was supported by an NSF EAR postdoctoral fellowship award (EAR-1725266). The authors thank Brian Gray for assistance with mixed modeling. Any use of trade, firm, or product names is for descriptive purposes only and does not imply endorsement by the U.S. Government.

References

Allen, A. P., Gillooly, J. F., & Brown, J. H. (2005). Linking the global carbon cycle to individual metabolism. *Functional Ecology*, *19*(2), 202–213. https://doi.org/10.1111/j.1365-2435.2005.00952.x

Amoros, C., & Bornette, G. (2002). Connectivity and biocomplexity in waterbodies of riverine floodplains. *Freshwater Biology*, *47*, 761–776. https://doi.org/10.1046/j.1365-2427.2002.00905.x

APHA. (2018). *Standard methods for the examination of water and wastewater* (23rd ed.). American Public Health Association.

Baines, S. B., Webster, K. E., Kratz, T. K., Carpenter, S. R., & Magnuson, J. J. (2000). Synchronous Behavior of temperature, calcium, and chlorophyll in lakes of Northern Wisconsin. *Ecology*, *81*(3), 815–825. https://doi.org/10.2307/177379

Barton, K., & Barton, M. K. (2013). *Package 'MuMIn' Version 1* (p. 18).

Beltaos, S. (2003). Threshold between mechanical and thermal breakup of river ice cover. *Cold Regions Science and Technology*, *37*(1), 1–13. https://doi.org/10.1016/S0165-232X(03)00010-7

Bouska, K. L., Houser, J. N., De Jager, N. R., & Hendrickson, J. (2018). Developing a shared understanding of the Upper Mississippi River: The foundation of an ecological resilience assessment. *Ecology and Society*, *23*(2). https://doi.org/10.5751/ES-10014-230206

Bouska, K. L., Houser, J. N., De Jager, N. R., Van Appledorn, M., & Rogala, J. T. (2019). Applying concepts of general resilience to large river ecosystems: A case study from the Upper Mississippi and Illinois rivers. *Ecological Indicators*, *101*, 1094–1110. https://doi.org/10.1016/j.ecolind.2019.02.002

Bukaveckas, P. A., MacDonald, A., Aufdenkampe, A., Chick, J. H., Havel, J. E., Schultz, R., et al. (2011). Phytoplankton abundance and contributions to suspended particulate matter in the Ohio, Upper Mississippi and Missouri Rivers. *Aquatic Sciences*, *73*(3), 419–436. https://doi.org/10.1007/s00027-011-0190-y

Burdis, R. M., DeLain, S. A., Lund, E. M., Moore, M. J. C., & Popp, W. A. (2020). Decadal trends and ecological shifts in backwater lakes of a large floodplain river: Upper Mississippi River. *Aquatic Sciences*, *82*(2). https://doi.org/10.1007/s00027-020-0703-7

Burnham, K. P., & Anderson, D. R. (2002). *Model selection and multimodel inference*. New York: Springer-Verlag.

Carey, J. C., Jankowski, K., Julian, P., Sethna, L. R., Thomas, P. K., & Rohweder, J. (2019). Exploring silica stoichiometry on a large floodplain riverscape. *Frontiers in Ecology and Evolution*, *7*. https://doi.org/10.3389/fevo.2019.00346

Cline, T. J., Schindler, D. E., Walsworth, T. E., French, D. W., & Lisi, P. J. (2020). Low snowpack reduces thermal response diversity among streams across a landscape. *Limnology and Oceanography Letters*, *5*(3), 254–263. https://doi.org/10.1002/lol2.10148

Cole, J. J., Caraco, N. F., & Peierls, B. L. (1992). Can phytoplankton maintain a positive carbon balance in a turbid, freshwater, tidal estuary? *Limnology and Oceanography*, *37*(8), 1608–1617. https://doi.org/10.4319/lo.1992.37.8.1608

Collins, S. M., Yuan, S., Tan, P. N., Oliver, S. K., Lapierre, J. F., Cheruvelil, K. S., et al. (2019). Winter precipitation and summer temperature predict lake water quality at macroscales. *Water Resources Research*, *55*(4), 2708–2721. https://doi.org/10.1029/2018WR023088

Contosta, A. R., Adolph, A., Burchsted, D., Burakowski, E., Green, M., Guerra, D., et al. (2017). A longer vernal window: The role of winter coldness and snowpack in driving spring transitions and lags. *Global Change Biology*, *23*(4), 1610–1625. https://doi.org/10.1111/gcb.13517

Cooley, S. W., & Pavelsky, T. M. (2016). Spatial and temporal patterns in Arctic river ice breakup revealed by automated ice detection from MODIS imagery. *Remote Sensing of Environment*, *175*, 310–322. https://doi.org/10.1016/j.rse.2016.01.004

Crawford, J. T., Loken, L. C., Stanley, E. H., Stets, E. G., Dornblaser, M. M., & Striegl, R. G. (2016). Basin scale controls on CO_2 and CH_4 emissions from the Upper Mississippi River: Mississippi River Greenhouse Gases. *Geophysical Research Letters*, *43*(5), 1973–1979. https://doi.org/10.1002/2015GL067599

De Jager, N. R., & Houser, J. N. (2012). Variation in water-mediated connectivity influences patch distributions of total N, total P, and TN:TP ratios in the Upper Mississippi River, USA. *Freshwater Science*, *31*(4), 1254–1272. https://doi.org/10.1899/12-035.1

De Jager, N. R., Rogala, J. T., Rohweder, J., Van Appledorn, M., Bouska, K. L., Houser, J. N., & Jankowski, K. J. (2018). *Indicators of ecosystem structure and function for the upper Mississippi river system* (Report no. 2018–1143) (p. 115). U.S. Geological Survey. https://doi.org/10.3133/ofr20181143

de Rham, L. P., Prowse, T. D., & Bonsal, B. R. (2008). Temporal variations in river-ice break-up over the Mackenzie River Basin, Canada. *Journal of Hydrology*, *349*(3–4), 441–454. https://doi.org/10.1016/j.jhydrol.2007.11.018

Decker, J. K., Wehr, J. D., Houser, J. N., & Richardson, W. B. (2015). Spatiotemporal phytoplankton patterns in the Upper Mississippi River in response to seasonal variation in discharge and other environmental factors. *River Systems*. https://doi.org/10.1127/rs/2015/0103

Escoffier, N., Bensoussan, N., Vilmin, L., Flipo, N., Rocher, V., David, A., et al. (2018). Estimating ecosystem metabolism from continuous multi-sensor measurements in the Seine River. *Environmental Science and Pollution Research*, *25*(24), 23451–23467. https://doi.org/10.1007/s11356-016-7096-0

Hall, R. O., Tank, J. L., Baker, M. A., Rosi-Marshall, E. J., & Hotchkiss, E. R. (2016). Metabolism, gas exchange, and carbon spiraling in rivers. *Ecosystems*, *19*(1), 73–86. https://doi.org/10.1007/s10021-015-9918-1

Hampton, S. E., Galloway, A. W. E., Powers, S. M., Ozersky, T., Woo, K. H., Batt, R. D., et al. (2017). Ecology under lake ice. *Ecology Letters*, *20*(1), 98–111. https://doi.org/10.1111/ele.12699

Hein, T., Baranyi, C., Heiler, G., Holarak, C., Riedler, P., & Schiemer, F. (1999). Hydrology as a major factor determining plankton development in two floodplain segments and the River Danube, Austria. *Archiv für Hydrobiologie*, *11*, 439–452. https://doi.org/10.1127/lr/11/1999/439

Hoeinghaus, D. J., Winemiller, K. O., & Agostinho, A. A. (2007). Landscape-scale hydrologic characteristics differentiate patterns of carbon flow in large-river food webs. *Ecosystems*, *10*(6), 1019–1033. https://doi.org/10.1007/s10021-007-9075-2

Holmes, E. E., Ward, E. J., & Scheuerell, M. D. (2014). *Analysis of multivariate time-series using the MARSS package*. MARSS User Guide.

Hotchkiss, E. R., Hall, R. O., Jr, Sponseller, R. A., Butman, D., Klaminder, J., Laudon, H., et al. (2015). Sources of and processes controlling CO_2 emissions change with the size of streams and rivers. *Nature Geoscience*, *8*(9), 696–699. https://doi.org/10.1038/ngeo2507

Houser, J. N. (2016). Contrasts between channels and backwaters in a large, floodplain river: Testing our understanding of nutrient cycling, phytoplankton abundance, and suspended solids dynamics. *Freshwater Science*, *35*(2), 457–473. https://doi.org/10.1086/686171

Houser, J. N., Bartsch, L. A., Richardson, W. B., Rogala, J. T., & Sullivan, J. F. (2015). Ecosystem metabolism and nutrient dynamics in the main channel and backwaters of the Upper Mississippi River. *Freshwater Biology*, *60*(9), 1863–1879. https://doi.org/10.1111/fwb.12617

Houser, J. N., Bierman, D. W., Burdis, R. M., & Soeken-Gittinger, L. A. (2010). Longitudinal trends and discontinuities in nutrients, chlorophyll, and suspended solids in the Upper Mississippi River: Implications for transport, processing, and export by large rivers. *Hydrobiologia*, *651*(1), 127–144. https://doi.org/10.1007/s10750-010-0282-z

Huusko, A., Greenberg, L., Stickler, M., Linnansaari, T., Nykänen, M., Vehanen, T., et al. (2007). Life in the ice lane: The winter ecology of stream salmonids. *River Research and Applications*, *23*(5), 469–491. https://doi.org/10.1002/rra.999

Hyrcik, A. R., & Stockwell, J. D. (2020). Under-ice mesocosms reveal the primacy of light but the importance of zooplankton in winter phytoplankton dynamics. *BioRxiv*. https://doi.org/10.1101/802819

Jane, S. F., Winslow, L. A., Remucal, C. K., & Rose, K. C. (2017). Long-term trends and synchrony in dissolved organic matter characteristics in Wisconsin, USA, lakes: Quality, not quantity, is highly sensitive to climate: Trends in DOM characteristics. *Journal of Geophysical Research: Biogeosciences*, *122*(3), 546–561. https://doi.org/10.1002/2016JG003630

Jankowski, K. J., Robinson, L., Kalas, J., Carhart, A., Lubinski, B., & Ruhser, J. (2020). *Mapping the thermal landscape of the upper Mississippi river* (Completion report no. LTRM-2017TL2). La Crosse, WI: U.S. Geological Survey.

Jewson, D. H., Granin, N. G., Zhdanov, A. A., & Gnatovsky, R. Y. (2009). Effect of snow depth on under-ice irradiance and growth of Aulacoseira baicalensis in Lake Baikal. *Aquatic Ecology*, *43*, 673–679. https://doi.org/10.1007/s10452-009-9267-2

Katz, S. L., Izmest'eva, L. R., Hampton, S. E., Ozersky, T., Shchapov, K., Moore, M. V., et al. (2015). The "Melosira years" of Lake Baikal: Winter environmental conditions at ice onset predict under-ice algal blooms in spring: Resolving Melosira years on Lake Baikal. *Limnology and Oceanography*, *60*(6), 1950–1964. https://doi.org/10.1002/lno.10143

Kendrick, M. R., & Huryn, A. D. (2015). Discharge, legacy effects and nutrient availability as determinants of temporal patterns in biofilm metabolism and accrual in an arctic river. *Freshwater Biology*, *60*(11), 2323–2336. https://doi.org/10.1111/fwb.12659

Kireta, A. R., Reavie, E. D., Sgro, G. V., Angradi, T. R., Bolgrien, D. W., Jicha, T. M., & Hill, B. H. (2012). Assessing the condition of the Missouri, Ohio, and Upper Mississippi rivers (USA) using diatom-based indicators. *Hydrobiologia*, *691*(1), 171–188. https://doi.org/10.1007/s10750-012-1067-3

Knights, B. C., Johnson, B. L., & Sandheinrich, M. B. (1995). Responses of bluegills and black crappies to dissolved oxygen, temperature, and current in Backwater Lakes of the Upper Mississippi River during winter. *North American Journal of Fisheries Management*, *15*, 390–399. https://doi.org/10.1577/1548-8675(1995)015<0390:robabc>2.3.co;2

Knowlton, M. F., & Jones, J. R. (1997). Trophic status of Missouri River floodplain lakes in relation to basin type and connectivity. *Wetlands*, *17*(4), 468–475. https://doi.org/10.1007/bf03161512

Lenth, R. (2018). Package 'lsmeans'. *The American Statistician*, *34*(4), 216–221.

Lottig, N. R., Tan, P.-N., Wagner, T., Cheruvelil, K. S., Soranno, P. A., Stanley, E. H., et al. (2017). Macroscale patterns of synchrony identify complex relationships among spatial and temporal ecosystem drivers. *Ecosphere*, *8*(12), e02024. https://doi.org/10.1002/ecs2.2024

Lubinski, K. (1993). *A conceptual model of the upper Mississippi river system ecosystem* (Technical report no. NTIS PB93-174357). Onalaska, WI: U.S. Fish and Wildlife Service.

Magee, M. R., & Wu, C. H. (2017). Effects of changing climate on ice cover in three morphometrically different lakes: Climate change on ice cover in three morphometrically different lakes. *Hydrological Processes*, *31*(2), 308–323. https://doi.org/10.1002/hyp.10996

Magnuson, J. J., Benson, B. J., & Kratz, T. K. (1990). Temporal coherence in the limnology of a suite of lakes in Wisconsin, U.S.A. *Freshwater Biology*, *23*, 145–159. https://doi.org/10.1111/j.1365-2427.1990.tb00259.x

Manier, J. T. (2015). *Spatial and temporal dynamics of phytoplankton assemblages in selected reaches of the Upper Mississippi River: Navigation Pools 8, 13 and 26*. (Masters Thesis). La Crosse, Wisconsin: University of Wisconsin La Crosse.

Manier, J. T., Haro, R. J., Houser, J. N., & Strauss, E. A. (2021). *Spatial and temporal dynamics of phytoplankton assemblages in the Upper Mississippi River*. (in press). River Research and Applications.

Marinos, R. E., Van Meter, K. J., & Basu, N. B. (2020). Is the river a chemostat? Scale versus land use controls on nitrate concentration-discharge dynamics in the Upper Mississippi River basin. *Geophysical Research Letters*, *47*(16). https://doi.org/10.1029/2020GL087051

Mejia, F. H., Fremier, A. K., Benjamin, J. R., Bellmore, J. R., Grimm, A. Z., Watson, G. A., & Newsom, M. (2019). Stream metabolism increases with drainage area and peaks asynchronously across a stream network. *Aquatic Sciences*, *81*(1). https://doi.org/10.1007/s00027-018-0606-z

Moore, M., Romano, S. P., & Cook, T. (2010). Synthesis of Upper Mississippi River System submersed and emergent aquatic vegetation: Past, present, and future. *Hydrobiologia*, *640*, 103–114. https://doi.org/10.1007/s10750-009-0062-9

Munoz, S. E., & Dee, S. G. (2017). El Niño increases the risk of lower Mississippi River flooding. *Scientific Reports*, *7*(1). https://doi.org/10.1038/s41598-017-01919-6

Nakagawa, S., & Schielzeth, H. (2013). A general and simple method for obtaining R^2 from generalized linear mixed-effects models. *Methods in Ecology and Evolution*, *4*(2), 133–142. https://doi.org/10.1111/j.2041-210x.2012.00261.x

Newton, B. W., Prowse, T. D., & de Rham, L. P. (2017). Hydro-climatic drivers of mid-winter break-up of river ice in western Canada and Alaska. *Hydrology Research*, *48*(4), 945–956. https://doi.org/10.2166/nh.2016.358

Nilsson, C., Polvi, L. E., & Lind, L. (2015). Extreme events in streams and rivers in arctic and subarctic regions in an uncertain future. *Freshwater Biology*, *60*(12), 2535–2546. https://doi.org/10.1111/fwb.12477

NOAA. (2021). *Multivariate ENSO index version 2 (MEI.v2)*. Retrieved from https://psl.noaa.gov/enso/mei/

Ochs, C. A., Pongruktham, O., & Zimba, P. V. (2013). Darkness at the break of noon: Phytoplankton production in the Lower Mississippi River. *Limnology and Oceanography*, *58*(2), 555–568. https://doi.org/10.4319/lo.2013.58.2.0555

Ohlberger, J., Scheuerell, M. D., & Schindler, D. E. (2016). Population coherence and environmental impacts across spatial scales: A case study of Chinook salmon. *Ecosphere*, *7*(4). https://doi.org/10.1002/ecs2.1333

Powers, S. M., Baulch, H. M., Hampton, S. E., Labou, S. G., Lottig, N. R., & Stanley, E. H. (2017). Nitrification contributes to winter oxygen depletion in seasonally frozen forested lakes. *Biogeochemistry*, *136*(2), 119–129. https://doi.org/10.1007/s10533-017-0382-1

Powers, S. M., & Hampton, S. E. (2017). Winter limnology as a new frontier. *Limnology and Oceanography Bulletin*, *25*(4), 103–108.

Prowse, T., Alfredsen, K., Beltaos, S., Bonsal, B., Duguay, C., Korhola, A., et al. (2011). Past and future changes in Arctic lake and river ice. *AMBIO*, *40*(S1), 53–62. https://doi.org/10.1007/s13280-011-0216-7

Rawlins, M. A., Cai, L., Stuefer, S. L., & Nicolsky, D. (2019). Changing characteristics of runoff and freshwater export from watersheds draining northern Alaska. *The Cryosphere*, *13*(12), 3337–3352. https://doi.org/10.5194/tc-13-3337-2019

R Core Team (2020). *R: A language and environment for statistical computing*. Vienna, Austria: R Foundation for Statistical Computing. https://www.R-project.org/

Reynolds, C. S., & Descy, J. P. (1996). The production, biomass, and structure of phytoplankton in large rivers. *Archiv Fur Hydrobiologie*, *10*, 161–187. https://doi.org/10.1127/lr/10/1996/161

Richardson, W. B., Strauss, E. A., Bartsch, L. A., Monroe, E. M., Cavanaugh, J. C., Vingum, L., & Soballe, D. M. (2004). Denitrification in the Upper Mississippi River: Rates, controls, and contribution to nitrate flux. *Canadian Journal of Fisheries and Aquatic Sciences*, *61*(7), 1102–1112. https://doi.org/10.1139/f04-062

Rokaya, P., Budhathoki, S., & Lindenschmidt, K.-E. (2018). Trends in the timing and magnitude of ice-jam floods in Canada. *Scientific Reports*, *8*(1). https://doi.org/10.1038/s41598-018-24057-z

Savoy, P., Appling, A. P., Heffernan, J. B., Stets, E. G., Read, J. S., Harvey, J. W., & Bernhardt, E. S. (2019). Metabolic rhythms in flowing waters: An approach for classifying river productivity regimes. *Limnology and Oceanography*, *64*(5), 1835–1851. https://doi.org/10.1002/lno.11154

Sellers, T., & Bukaveckas, P. A. (2003). Phytoplankton production in a large, regulated river: A modeling and mass balance assessment. *Limnology & Oceanography*, *48*(4), 1476–1487. https://doi.org/10.4319/lo.2003.48.4.1476

Sharma, S., Blagrave, K., Magnuson, J. J., O'Reilly, C. M., Oliver, S., Batt, R. D., et al. (2019). Widespread loss of lake ice around the Northern Hemisphere in a warming world. *Nature Climate Change*, *9*(3), 227–231. https://doi.org/10.1038/s41558-018-0393-5

Sharma, S., Magnuson, J. J., Batt, R. D., Winslow, L. A., Korhonen, J., & Aono, Y. (2016). Direct observations of ice seasonality reveal changes in climate over the past 320–570 years. *Scientific Reports*, *6*(1). https://doi.org/10.1038/srep25061

Sharma, S., Meyer, M. F., Culpepper, J., Yang, X., Hampton, S., Berger, S. A., et al. (2020). Integrating perspectives in understanding lake ice dynamics in a changing world. *Journal of Geophysical Research: Biogeosciences*, *125*. https://doi.org/10.1029/2020JG005799

Shiklomanov, A. I., & Lammers, R. B. (2014). River ice responses to a warming Arctic—Recent evidence from Russian rivers. *Environmental Research Letters*, *9*(3), 035008. https://doi.org/10.1088/1748-9326/9/3/035008

Smits, A. P., Ruffing, C. M., Royer, T. V., Appling, A. P., Griffiths, N. A., Bellmore, R., et al. (2019). Detecting signals of large-scale climate phenomena in discharge and nutrient loads in the Mississippi-Atchafalaya River basin. *Geophysical Research Letters*, *46*(7), 3791–3801. https://doi.org/10.1029/2018GL081166

Soballe, D. M., & Fischer, J. R. (2004). *Long term resource monitoring program procedures: Water quality monitoring* (p. 73). La Crosse, WI: U.S. Geological Survey Upper Midwest Environmental Sciences Center.

Soranno, P. A., Wagner, T., Collins, S. M., Lapierre, J., Lottig, N. R., & Oliver, S. K. (2019). Spatial and temporal variation of ecosystem properties at macroscales. *Ecology Letters*, *22*(10), 1587–1598. https://doi.org/10.1111/ele.13346

Sparks, R. E. (1995). Maintaining and restoring the ecological integrity of the Mississippi River: Importance of floodplains and floodpulses. In *Transactions of the 60th North American wildlife and natural resources conference* (p. 8). Minneapolis, MN: U.S. Geological Survey Environmental Management Technical Center.

Sparks, R. E., Nelson, J. C., & Yin, Y. (1998). Naturalization of the flood regime in regulated rivers: The case of the Upper Mississippi River. *Bioscience*, *48*(9), 706–720. https://doi.org/10.2307/1313334

Thellman, A., Jankowski, K. J., Hayden, B., Yang, X., Dolan, W., Smits, A. P., & O'sullivan, A. M. (2021). The ecology of river ice. *JGR-Biogeosciences*, In press.

Thorp, J. H., & Delong, M. D. (1994). The riverine productivity model: An heuristic view of carbon sources and organic processing in large river ecosystems. *Oikos*, *70*(2), 305. https://doi.org/10.2307/3545642

Tremblay, P., Leconte, R., Jay Lacey, R. W., & Bergeron, N. (2014). Multi-day anchor ice cycles and bedload transport in a gravel-bed stream. *Journal of Hydrology*, *519*, 364–375. https://doi.org/10.1016/j.jhydrol.2014.06.036

Turcotte, B., & Morse, B. (2013). A global river ice classification model. *Journal of Hydrology*, *507*, 134–148. https://doi.org/10.1016/j.jhydrol.2013.10.032

Turcotte, B., & Morse, B. (2017). The winter environmental continuum of two watersheds. *Water*, *9*(5), 337. https://doi.org/10.3390/w9050337

Turcotte, B., Morse, B., Bergeron, N. E., & Roy, A. G. (2011). Sediment transport in ice-affected rivers. *Journal of Hydrology*, *409*(1–2), 561–577. https://doi.org/10.1016/j.jhydrol.2011.08.009

Twine, T. E., Kucharik, C. J., & Foley, J. A. (2005). Effects of El Niño–Southern Oscillation on the climate, water balance, and streamflow of the Mississippi River Basin. *Journal of Climate*, *18*, 4840–4861. https://doi.org/10.1175/jcli3566.1

Twiss, M. R., McKay, R. M. L., Bourbonniere, R. A., Bullerjahn, G. S., Carrick, H. J., Smith, R. E. H., et al. (2012). Diatoms abound in ice-covered Lake Erie: An investigation of offshore winter limnology in Lake Erie over the period 2007 to 2010. *Journal of Great Lakes Research*, *38*(1), 18–30. https://doi.org/10.1016/j.jglr.2011.12.008

Twiss, M. R., Smith, D. E., Cafferty, E. M., & Carrick, H. J. (2014). Phytoplankton growth dynamics in offshore Lake Erie during mid-winter. *Journal of Great Lakes Research*, *40*(2), 449–454. https://doi.org/10.1016/j.jglr.2014.03.010

Uehlinger, U. (2006). Annual cycle and inter-annual variability of gross primary production and ecosystem respiration in a floodprone river during a 15-year period. *Freshwater Biology*, *51*(5), 938–950. https://doi.org/10.1111/j.1365-2427.2006.01551.x

Uehlinger, U., Konig, C., & Reichart, P. (2000). Variability of photosynthesis±irradiance curves and ecosystem respiration in a small river. *Freshwater Biology*, *44*, 493–507. https://doi.org/10.1046/j.1365-2427.2000.00602.x

Uehlinger, U., & Naegeli, M. W. (1998). Ecosystem Metabolism, Disturbance, and Stability in a Prealpine Gravel Bed River. *Journal of the North American Benthological Society*, *17*(2), 165–178. https://doi.org/10.2307/1467960

USACE. (2011). *Upper Mississippi river system ecosystem Restoration Objectives*. U.S. Army Corps of Engineers. Retrieved from http://www.mvr.usace.army.mil/Portals/48/docs/Environmental/EMP/UMRR_Ecosystem_Restoration_Objectives_2009.pdf

USGCRP. (2017). Climate Science Special Report: Fourth National Climate Assessment (Vol. I, p. 470). Washington D.C: U.S. Global Change Research Program. https://doi.org/10.7930/J0J964J6

U.S. Geological Survey (2021). National Water Information System data available on the World Wide Web (USGS Water Data for the Nation). http://waterdata.usgs.gov/nwis/

Van den Briink, F. W. B., de Leeuw, J. P. H. M., van der Velde, G., & Verheggen, G. M. (1993). Impact of hydrology on the chemistry and phytoplankton development in floodplain lakes along the Lower Rhine and Meuse. *Biogeochemistry*, *19*, 103–128.

Ward, J. V., Tockner, K., Arscott, D. B., & Claret, C. (2002). Riverine landscape diversity. *Freshwater Biology*, *47*, 517–539. https://doi.org/10.1046/j.1365-2427.2002.00893.x

Weber, C., Nilsson, C., Lind, L., Alfredsen, K. T., & Polvi, L. E. (2013). Winter disturbances and riverine fish in temperate and cold regions. *BioScience*, *63*(3), 199–210. https://doi.org/10.1525/bio.2013.63.3.8

Webster, K. E., Soranno, P. A., Baines, S. B., Kratz, T. K., Bowser, C. J., Dillon, P. J., et al. (2000). Structuring features of lake districts: Landscape controls on lake chemical responses to drought. *Freshwater Biology*, *43*, 499–515. https://doi.org/10.1046/j.1365-2427.2000.00571.x

Wiens, J. A. (2002). Riverine landscapes: Taking landscape ecology into the water. *Freshwater Biology*, *47*, 501–515. https://doi.org/10.1046/j.1365-2427.2002.00887.x

Yang, X., Pavelsky, T. M., & Allen, G. H. (2020). The past and future of global river ice. *Nature*, *577*(7788), 69–73. https://doi.org/10.1038/s41586-019-1848-1

Zuur, A. F., Fryer, R. J., Jolliffe, I. T., Dekker, R., & Beukema, J. J. (2003). Estimating common trends in multivariate time series using dynamic factor analysis. *Environmetrics*, *14*, 542–552. https://doi.org/10.1139/f03-030